ELSEVIER

Surface and Coatings Technology 151–152 (2002) 133–137

SURFACE & COATINGS TECHNOLOGY

www.elsevier.com/locate/surfcoat

Structure of amorphous carbon-nitride thin films

G. Radnóczi*, I. Kovács, O. Geszti, L.P. Bíró, G. Sáfrán

Research Institute for Technical Physics and Materials Science, Hungarian Academy of Sciences, Konkoly-Thege út 29-33, P.O. Box 49, Budapest 1121, Hungary

Abstract

CN_x thin films were prepared in high vacuum by evaporation of C from a pair of graphite rods in a DC arc ignited in N_2 at pressures of up to 1 mbar onto NaCl, Highly ordered pyrolytic graphite (HOPG) and Si substrates. The substrate temperature varied between room temperature and 800 °C. The effect of deposition temperature and N_2 gas pressure on the morphology, structure, composition and electrical properties of CN_x thin films was studied by high-resolution transmission electron microscopy (HRTEM), X-ray microanalysis (EDS), and scanning tunneling microscopy and spectroscopy (STM and STS). Morphology ranging from homogeneous layers through spherical or cylindrical particles embedded into the films to low-density globular deposits of CN_x was observed as a function of the applied N_2 gas pressure. The N composition found was between 1 and 20 at.% and the structure varied from amorphous through fullerene-like to nanocrystalline diamond composed of amorphous CN_x, depending on the temperature and the plasma parameters. The behavior of the films during heat treatment was recorded by electrical conductivity measurements. The activation energy of electrical conductivity was found to be 0.18 eV for carbon and 0.38 eV for CN_x films and was independent of the deposition temperature.

Keywords: Carbon nitride; Structure; Electrical conductivity; Electron microscopy; Scanning tunneling microscopy; Scanning tunneling spectroscopy

1. Introduction

The predicted C_3N_4 compound of high hardness and toughness [1] could be a promising candidate for hard coatings and tribological applications. Either the stoichiometric form or various compositions of CN_x thin films might be of high technological and scientific interest. Some CN_x films were found to have a distorted graphite-like structure consisting of buckled sp^2-hybridized CN_x planes cross-linked by sp^3-hybridized bonds [2]. The buckling is attributed to the incorporation of pentagons into the basal planes of the graphite-like structure, due to the presence of N atoms. Tetragonal and graphite-like atomic configurations can be characterized by their specific electrical properties [3–6]. In our experiments CN_x films were prepared by the interaction of carbon vapor generated by a DC arc between two graphite rods and nitrogen plasma. The structure and electrical conductivity were studied to characterize the films.

* Corresponding author. Tel.: +36-12754980; fax: +36-12754996.
E-mail address: radnoczi@mfa.kfki.hu (G. Radnóczi).

2. Experiment

CN_x thin films were prepared in high vacuum by evaporation of C from a pair of graphite rods in a DC arc kept in N_2 at pressure of up to 1 mbar onto (100) Si, NaCl, HOPG and quartz plates between room temperature and 800 °C. An additional DC plasma was ignited above the substrate in some experiments. The samples were characterized by transmission and high-resolution electron microscopy (TEM and HREM), X-ray microanalysis (EDS) [7], scanning tunneling microscopy- and spectroscopy (STEM and STS) and electrical conductivity measurements.

3. Results and discussion

The structure of the films varies with the deposition parameters. The amorphous carbon layer deposited at room temperature displays a rather homogeneous structure (Fig. 1). In comparison, a CN_x film, also deposited at room temperature and at 0.05 mbar N_2 pressure, shows an inhomogeneous structure, containing voids, columns, walls and embedded particles, probably form-

0257-8972/01/$ - see front matter
PII: S0257-8972(01)01626-7

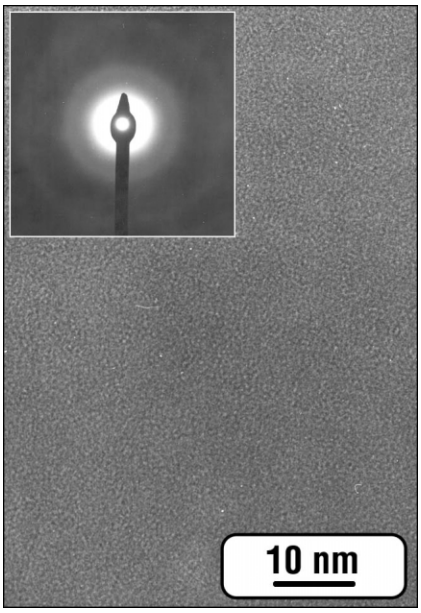

Fig. 1. Plan-view bright-field TEM image of 30-nm-thick C film deposited at room temperature on NaCl substrate.

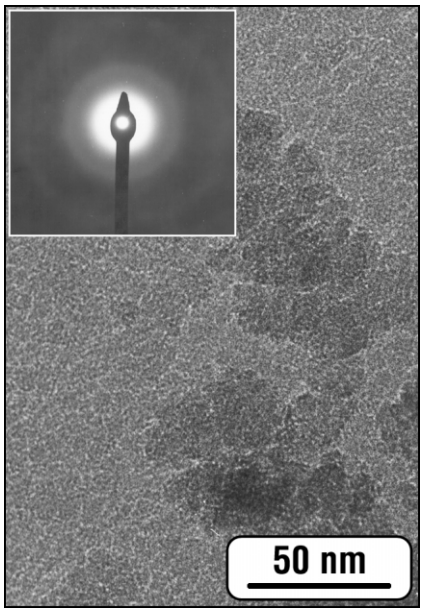

Fig. 2. Plan-view bright-field TEM image of 30-nm-thick CN_x film deposited at room temperature and N_2 pressure 0.05 mbar.

ing in the atmosphere due to the collision of carbon atoms (Fig. 2). According to EDS measurements, this film contains 1.5 at.% nitrogen.

CN_x films prepared under nearly the same conditions (0.08 mbar N_2 pressure), but with a plasma ignited between the carbon source and the substrate, contain significantly more nitrogen (5–10 at.%); their structure is more homogeneous, without columns and particles. Some ordering can be recognized in the structure in HREM, in the form of small domains, showing a few curved graphite-like planes (area marked by circles in Fig. 3).

Films grown at elevated temperature (800 °C, without the additional plasma) show a nanocrystalline composite structure, consisting of an amorphous matrix and nanocrystallites, giving just two rings in the selected-area diffraction pattern (Fig. 4). These correspond to diamond 111 and 220 reflections. They are definitely sharper than the diffraction rings obtained from all three layers shown in Figs. 1–3. Nanocrystallinity was also proved in the high-temperature films by dark-field imaging. According to this, the shape of the crystallites is elongated, having a diameter of approximately 1 nm and a length of approximately 10 nm. The nitrogen content in the films deposited at 800 °C is low, and remains below the detection limit for EDS (approx. 1%). This ordering of the structure, approaching the nano-composite state, can be observed in layers grown at substrate temperatures above 600 °C.

For electronic characterization, STS measurements of the CN_x films were carried out. A comparison of the STS $I–V$ curve of a CN_x layer, possessing a structure similar to that shown in Fig. 2, to that of HOPG, showing a semi-metallic character, is shown in Fig. 5. The STS $I–V$ measurements revealed a bandgap of approximately 1 eV in the a-CN_x layer, which is characteristic of a-C and CN_x films [4,5,8,9].

The electrical resistance of the CN_x films shows an Arrhenius-type of temperature dependence in all cases, which is similar to, but more linear than that observed

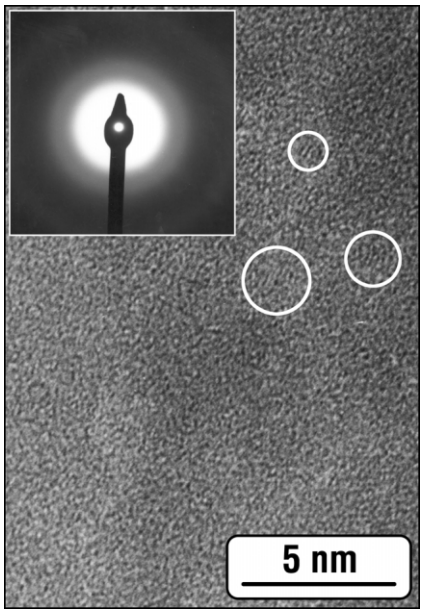

Fig. 3. Plan-view bright-field TEM image of 60-nm-thick CN_x film deposited at a temperature of 70 °C and N_2 pressure of 0.08 mbar on a Si substrate.

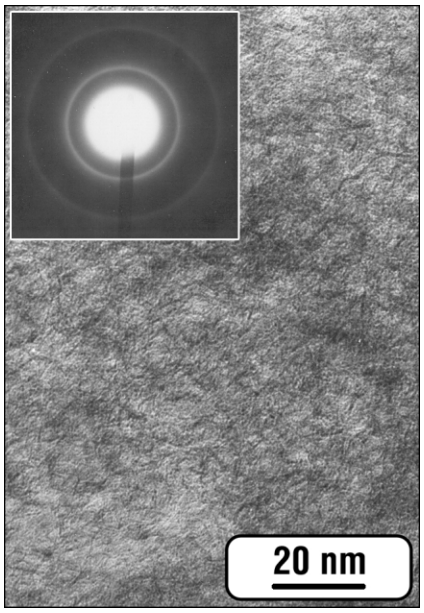

Fig. 4. Plan-view bright-field TEM image of 60-nm-thick CN_x film deposited at a temperature of 800 °C and N_2 pressure of 0.05 mbar on a Si substrate.

in [10]. In the interpretation of the results, we followed the theory developed by Mott and Davis [11]. Fig. 6 shows the $\ln(R) = f(1000/T)$ plot of a pure carbon film, where R is the resistance measured for the film. Only two regions in the Arrhenius plot can be separated — the first corresponding to the low- and the second to the high-temperature processes, with activation energy $E_{a1} =$ 0.01–0.03 and $E_{a2} = 0.18$ eV, respectively.

In our calculations, we neglected the Poole–Frenkel effect because the correction would be less then 1.7×10^{-3} eV (assuming $\varepsilon = 10$ [12,13]). The first region is related to the excitation of charge carriers in the zone of high mobility. The second region is related to conduction by carriers in the localized states and characterized by the activation energy of jumping from

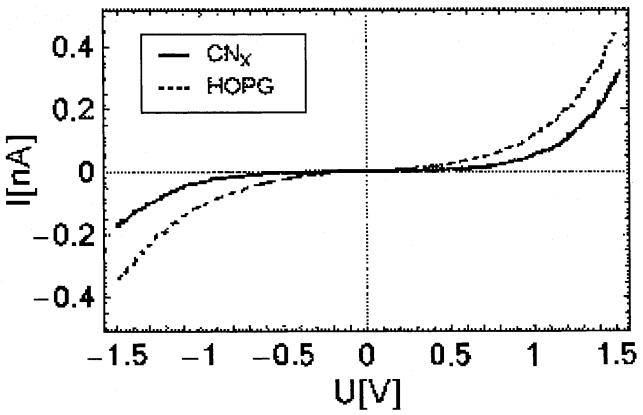

Fig. 5. STS I–V measurement of the CN_x film, compared to HOPG.

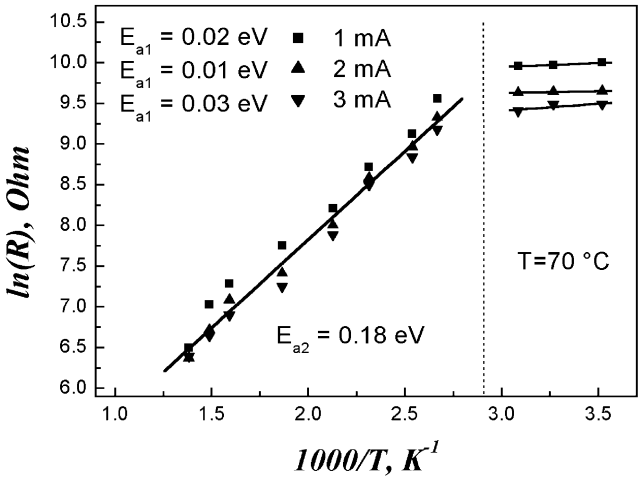

Fig. 6. Temperature dependence of the electrical resistance of 30-nm-thick C film deposited at room temperature.

one defect to another in the nearest neighborhood. The transition temperature is approximately 70 °C.

In the TEM image shown in Fig. 2, the CN_x film structure is amorphous, but different from pure carbon. In this film, a large number of defects were observed, which means that localized states with a wide range of energy values must exist in the bandgap. Therefore, the low-temperature region in Fig. 7 cannot be interpreted as clearly. The high-temperature range, as in the case of pure carbon films, is related to conductance by carriers excited to the high-mobility zone. The activation energy obtained from the plot for this film is 0.38 eV.

In the plot shown in Fig. 8, we can separate all three processes that are characteristic for amorphous semiconductors. The low-temperature region corresponds to jumping between localized states near the Fermi level, with activation energy close to kT. The middle region,

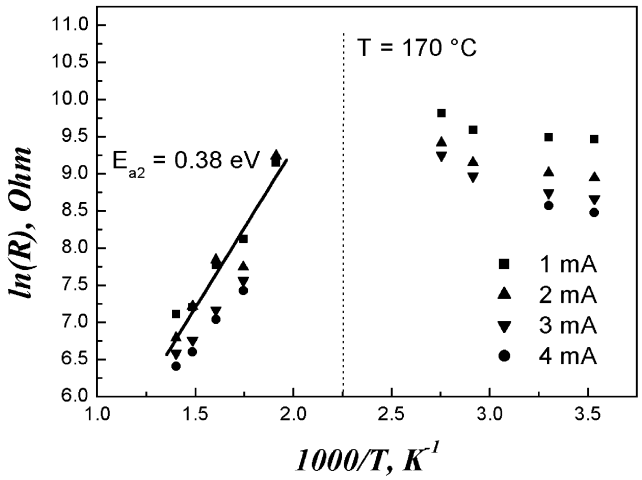

Fig. 7. Temperature dependence of the electrical resistance of 30-nm-thick CN_x film on Si substrate deposited at room temperature and N_2 pressure of 0.05 mbar.

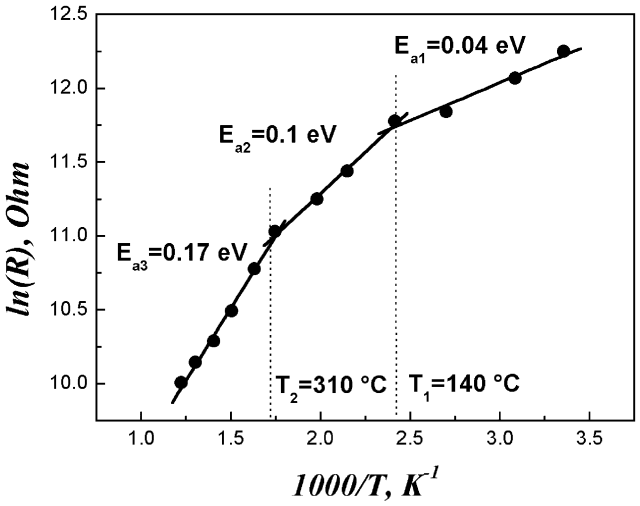

Fig. 8. Temperature dependence of the electrical resistance of 60-nm-thick CN_x film on Si substrate deposited at a temperature of 70 °C and N_2 pressure of 0.08 mbar.

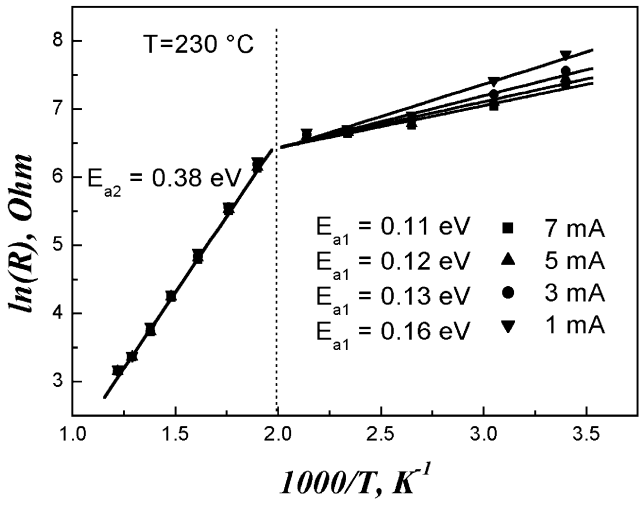

Fig. 9. Temperature dependence of the electrical resistance of 60-nm-thick CN_x film on Si substrate deposited at a temperature of 800 °C and N_2 pressure of 0.05 mbar.

which was not observed in other samples, corresponds to excitation of charge carriers to the zone of low mobility and to jumping between localized states. The activation energy for these processes is approximately 0.1 eV. Processes observed at high temperature correspond to excitation to a zone of high mobility, with an activation energy of 0.17 eV.

In Fig. 9, the behavior of CN_x film deposited at 800 °C and 0.05 mbar N_2 pressure is shown. The two regions can also be separated on the plot of $\ln(R)=f(1000/T)$: first, the low-temperature range between room temperature and 230 °C (the transition temperature in this case) with activation energy $E_{a1}=0.11-0.16$ eV, and second, the high-temperature range between 230 and 550 °C with activation energy $E_{a2}=0.38$ eV. The activation energy measured at lower temperatures is the sum of two values: the energy of excitation of charge carriers in localized states and the energy of carriers jumping between localized states. The latter must be approximately kT, which is 0.02–0.04 eV in this range. Therefore, the zone of localized states is approximately 0.1 eV.

4. Conclusions

Structural and electrical characterization of amorphous C and CN_x films has been carried out. The activation energy of electrical conductivity was calculated from the temperature dependence of the electrical resistance of the films. As a result of the investigation, a correlation was found between the microstructure of the films and the mobility bandgap of the charge carriers.

The structure of all films was amorphous and the electrical resistance showed semiconductor-like behavior. The activation energy calculated from high-temperature data was found to be 0.38 eV for films with various kinds of structural defects (phase boundaries, column boundaries, dangling bonds) and 0.17–0.18 eV for films with a homogeneous structure and low density of defects.

The behavior of the electrical resistance at low temperature was not as clear: both semiconductor- and metallic-like temperature dependence has been observed. It can be concluded that in this temperature interval, the conductivity of the films is more sensitive to deposition and structural parameters.

Concerning the structure of the films, the films become more ordered with increasing N_2 content. Increasing the substrate temperature leads to ordering and the formation of diamond nanocrystals with a whisker-like shape at 800 °C.

Acknowledgements

This work was carried out within the co-operation of the TMR project FMRX-CT97-0103 and was financially supported by projects OMFB EU-98-B4/145, OTKA T030424 and T030435, and by the EU under contract number ICAI-CT-2000-70029.

References

[1] A.M. Liu, M.L. Cohen, Science 245 (1989) 841.
[2] H. Sjöström, S. Stafström, M. Boman, J.-E. Sundgren, Phys. Rev. Lett. 75 (1995) 1336.
[3] E. Broitman, N. Hellgren, K. Järrendahl, et al., J. Appl. Phys. 89 (2) (2001) 1184–1190.
[4] A. Wei, D. Chen, N. Ke, W.Y. Cheung, S. Peng, S.P. Wong:, J. Phys. D: Appl. Phys. 31 (1998) 1522–1526.

[5] N. Lin, N. Hellgren, M.P. Johansson, L. Hultman, R. Erlandson, J.-E. Sundgren, Phys. Rev. B 61 (2000) 4898.
[6] Y.F. Lu, Z.M. Ren, W.D. Song, et al., J. Appl. Phys. 84 (5) (1998) 2909.
[7] G. Sáfrán, I. Kovács, O. Geszti, I. Bertóti, G. Radnóczi, in: K. Kovács (Ed.), Proceedings of the IVth Multinational Congress on Electron Microscopy, Veszprém, Hungary, September 1999, 1999, p. 361.
[8] G. Radnóczi, G. Sáfrán, I. Kovács, O. Geszti, L. Bíró, Acta Phys. Slov. 50 (6) (2000) 679–684.
[9] F.Y. Chuang, C.Y. Sun, T.T. Chen, I.N. Lin, Appl. Phys. Lett. 69 (1995) 3504.
[10] M.A. Monclus, D.C. Cameron, A.K.M.S. Chowdhurry, Thin Solid Films 341 (1999) 94–100.
[11] N.F. Mott, E.A. Davis, Electron Processes in Non-Crystalline Materials, Clarendon Press, Oxford, 1979.
[12] K.W. Boer, Survey of Semiconductor Physics, Van Nostrand Reinhold, New York, 1990.
[13] C. Popov, L.M. Zambov, M.F. Plass, W. Kulisch, Thin Solid Films 377/378 (2000) 156.